Title

Controlled Vertical Transfer of Individual Au Atoms Using a Surface Supported Carbon Radical for Atomically Precise Manufacturing

Journal

Precision Chemistry, 1(2)

ISSN

2771-9316

Authors

Bothra, Pallavi
Stieg, Adam Z
Gimzewski, James K
et al.

Publication Date

2023-04-24

DOI

10.1021/prechem.3c00011

ACS Partner Journal
PRECISION CHEMISTRY
pubs.acs.org/PrecisionChem
Article

Controlled Vertical Transfer of Individual Au Atoms Using a Surface Supported Carbon Radical for Atomically Precise Manufacturing

Pallavi Bothra, Adam Z. Stieg, James K. Gimzewski, and Philippe Sautet*

Cite This: *Precis. Chem.* 2023, 1, 119−126

ABSTRACT: To explore a proof-of-concept for atomically precise manufacturing (APM) using scanning probe microscopy (SPM), first principle theoretical calculations of atom-by-atom transfer from the apex of an SPM tip to an individual radical on a surface-bound organic molecule have been performed. Atom transfer is achieved by spatially controlled motion of a gold terminated tip to the radical. Two molecular tools for SPM-based APM have been designed and investigated, each comprising an adamantane core, a radical end group, and trithiol linkers to enable strong chemisorption on the Au(111) surface: ethynyl-adamantane-trithiol and adamantyl-trithiol. We demonstrate the details of controlled Au atom abstraction during tip approach toward and retraction from the radical species. Upon approach of the tip, the apical Au atom undergoes a transfer toward the carbon radical at a clearly defined threshold separation. This atomic displacement is accompanied by a net energy gain of the system in the range −0.5 to −1.5 eV, depending on the radical structure. In the case of a triangular pyramidal apex model, two tip configurations are possible after the tip atom displacement: (1) an Au atom is abstracted from the tip and bound to the C radical, not bound to the tip base anymore, and (2) apical tip atoms rearrange to form a continuous neck between the tip and radical. In the second case, subsequent tip retraction leads to the same final configuration as the first, with the abstracted Au atom bound to radical carbon atom of the molecular tool. For the less reactive adamantyl-trithiol radical molecular tool, Au atom transfer is less energetically favored, but this has the advantage of avoiding other apex gold atoms from rearrangement.

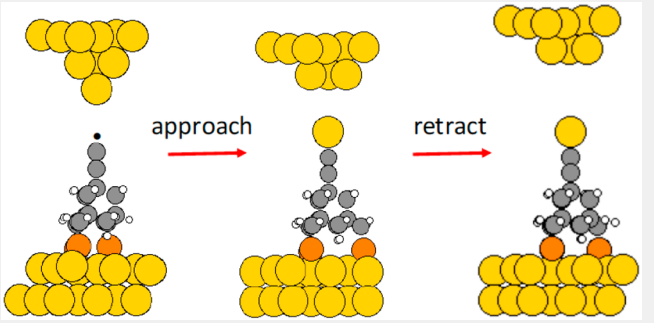

KEYWORDS: *atomically precise manufacturing, scanning probe microscopy, density functional theory, atom vertical transfer, molecular radical*

INTRODUCTION

Atomically precise manufacturing offers an opportunity to manufacture defect-free materials, components, and systems from individual atoms and molecules. While no laws of physics or chemistry exclude realization of this disruptive technology and its potential to create paradigm shifts in engineering, medicine, and information technology, APM remains an enormous scientific challenge. Advances in nanotechnology enabled by the integration of synthetic chemistry, theoretical modeling, and SPM-based methods provide a pathway to the robust production of atomically precise structures. To date, repositioning of both surface-bound atoms and molecules and induction of chemical reactions with and between them has been successfully demonstrated in two dimensions with a variety of atomic and molecular systems. One example domain where APM could be employed is the surface engineering of metals, since this is a central domain to many applications. With the size decrease of the devices or function in microelectronic applications, for example, smaller scales of modifications of metals by deposit or etching are required. The ultimate scale deals with the engineered manipulation of metal surfaces atom by atom.[1,2] Placing or removing atoms at precise locations is a grand challenge and an inspiration for researchers following the vision of Feynman on nanotechnology. Such atomically precise manufacturing would be a clear change of paradigm in our manufacturing processes.[3,4]

The controlled abstraction, or removal, and transfer of a single atom represents an enabling fundamental first step toward the realization of APM in three dimensions. Scanning tunneling microscopy has previously been used to manipulate single atomic adsorbates following the pioneering work of Don Eigler and colleagues positioning Xe atoms with atomic precision on a Ni surface.[2] Reversible vertical manipulation

Received: January 24, 2023
Revised: March 21, 2023
Accepted: March 22, 2023
Published: March 30, 2023

https://doi.org/10.1021/prechem.3c00011
Precis. Chem. 2023, 1, 119−126

between surface and tip of Xe atoms or propene molecules on Cu(211) and of CO on Cu(111) has been realized by Rieder and colleagues.[5,6] Individual Ge atoms were extracted from a Ge(111) surface using tip−surface contact with a STM at zero bias voltage by Dujardin and colleagues.[7] A near contact atomic force microscope has also been used for vertical abstraction of atoms from a Si(111) 7 × 7 surface. A central example of application is the controlled removal of single hydrogen atoms from the H:Si(100) surface to realize hydrogen resist lithography on H:Si (100) surfaces with single atom specificity.[8−10] To explore the feasibility of utilizing designed molecular tools for atomic abstraction through mechanochemical means, the present work seeks to model the sculpting of a metallic tip structure through controlled removal of individual metal atoms using reactive adsorbates, following the process shown in Figure 1.

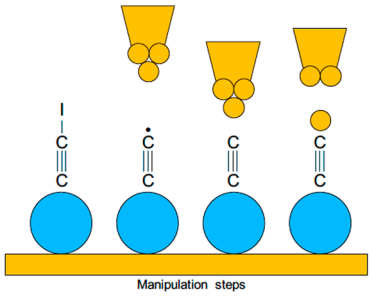

Figure 1. Schematic representation of atomic manipulation using surface-bound molecular radicals. A representative molecular tool (iodo-ethynyl-adamantanetrithiol) is supported on an Au surface. Cleavage of the C−I bond produces a radical center on the uppermost carbon atom. As the gold tip approaches the radical, a single gold atom is spontaneously abstracted from the tip and transferred to the radical. The modified tip is then retracted from the surface.

The tip is envisaged to be of the type used in SPM, thereby offering the requisite positioning accuracy to bring the apical tip atom in close proximity a surface where highly chemically active molecules are placed. While fundamental in nature, validation of tip-based mechanochemical concepts through simulation and modeling opens the door to the experimental realization of atomically controlled etching, or subtractive preparation of well-defined metallic shapes. This mechano-chemical approach also offers the possibility to produce atomically defined tip structures in situ before and/or during SPM experiments, including high-resolution imaging or manipulation of molecular objects, which critically depend on the structure of the tip apex. That tip apex atomic structure is often not known in SPM experiments, but approaches have been developed using adsorbates as CO that enable the characterization of the tip apex and in some cases the individual resolution of its atoms.[11,12]

Here, we consider two organic molecules adsorbed on the Au(111) surface via three thiol groups and bearing a carbon radical center as shown in Scheme 1. Cleavage of the terminal C−I bond, either photoinduced or by inelastic tunneling using voltage pulses applied by the SPM tip, can produce the desired carbon radical at the end of the molecule.[5] These radicals have the potential to bind to a metal atom from a Au tip approached toward them and, if the tip is retracted away from the surface, to abstract the Au atom from the tip. Many questions remain open for such single atom manipulation. Will the metal atom

Scheme 1. Representation of the Two Au Surface-Bound Molecular Radicals Considered Here: Ethynyl-Adamantane-Trithiol (Left) and Adamantyl-Trithiol (Right)[a]

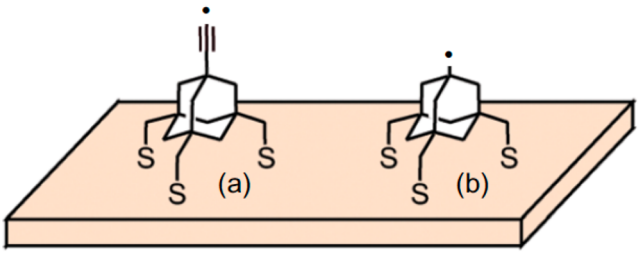

[a]Adapted with permission from ref 24. Copyright (2013) Royal Society of Chemistry.

abstraction occur? Will instead the Au tip be deformed in a ductile way? At what distance between the radical and the tip will the bond be formed? How accurate should the placement of the tip be parallel to the surface for a controlled abstraction of a given atom? Finally, how is the result dependent on the molecular structure of the C radical? We address these questions herein, using first principle calculations based on density functional theory.

COMPUTATIONAL METHODS AND MODELS

Plane wave DFT calculations were performed using the projector augmented wave method provided in the Vienna ab initio simulation package (VASP).[13] The Perdew−Burke−Ernzerhof (PBE) exchange-correlation functional[14] with a plane wave expansion cutoff of 400 eV and modeled dispersion interactions using the DFT-D3 method developed by Grimme et al. was used.[15] Four layers were used to model the Au(111) surface. The bottom two layers are fixed, but all other atoms are allowed to relax during the calculations until the forces are less than 0.05 eV/Å. A vacuum spacing of ∼12 Å was included, which is sufficient to minimize the periodic interaction in the surface normal direction. In terms of system size, a 3 × 3 unit cell with a corresponding Monkhorst−Pack k-point mesh of 4 × 4 × 1 is employed. For the tip, 5 layers were considered with the top two layers fixed. Two types of tips have been modeled as shown in Figure 2: (1) a sharp tip with a single atom at the apex (Figure 2a) and (2) a

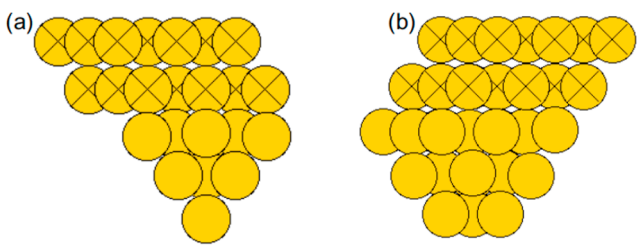

Figure 2. Structural models of tip shapes: (a) a sharp tip with a single Au atom at the apex and (b) a blunt tip with 3 Au atoms at the apex.

flat tip with 3 Au atoms at the apex (Figure 2b). While SPM tips are typically made of W or a PtIr alloy, unavoidable and/or intentional contact between the tip and surface results in transfer of an ensemble of Au atoms at the apex of the tip. As such, Au tips were employed.

RESULTS AND DISCUSSION

a. Adsorption of Iodo-Ethynyl-Adamantanetrithiol on the Au(111) Surface

The interaction between alkyl-thiols and Au surfaces has been well documented,[16−18] whereby alkyl-thiols bind to Au via the

https://doi.org/10.1021/prechem.3c00011
Precis. Chem. 2023, 1, 119−126

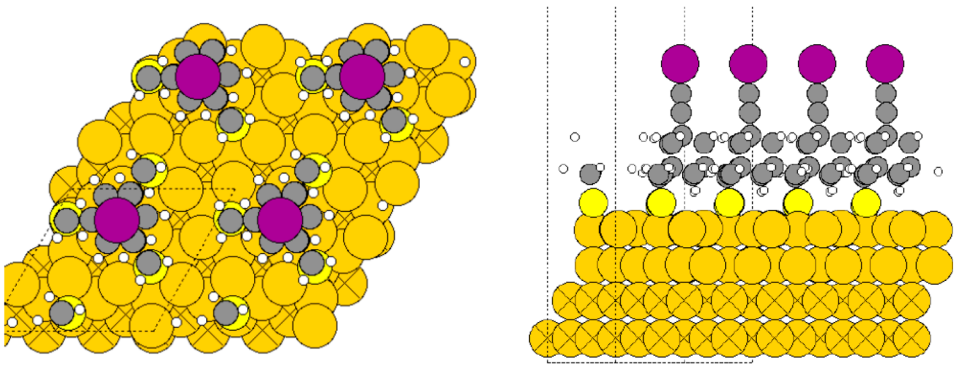

Figure 3. Top (left) and side (right) view of the calculated (3 × 3) adsorption structure of iodo-ethynyl-adamantanetrithiol chemisorbed on the Au(111) surface. Au: gold; S: yellow; C: gray; H: white, I: purple.

S atom after cleavage of the S−H bond.[19−22] Similarly, the adamantanetrithiol unit binds to Au(111) via each of its 3 S atoms as shown by previous STM and DFT studies.[23,24] The calculated binding energy of the triply dehydrogenated adamantane unit on Au (501 kJ mol^{-1}) is consistent with the previous experimental and theoretical studies. This strong bonding between the molecule and the Au(111) surface produces very stable chemisorption, the structure of which is shown in Figure 3. Sulfur atoms are found to bind at hollow sites on the Au(111) surface. Decomposition of the adsorbed molecule through either photoexcitation or inelastic tunneling is assumed to cleave the C−I bond in an homolytic manner, resulting in a terminal carbon radical.[5]

b. Atomic Abstraction Trajectories from the Sharp Tip Model with the Ethynyl-Adamantane-Trithiol Radical

Approach of the sharp Au tip toward the supported ethynyl-adamantane-trithiol radical was utilized to examine how the radical moiety promotes Au atom abstraction and metal−metal bond breaking at the Au tip. The interaction energy between the tip and the surface-mounted molecular tool has been systematically explored by changing the tip−surface separation (Figure 4), which enabled the elucidation of structural models throughout the mechanochemical abstraction process (Figure 5). Calculations combine multiple geometry optimization starting from an initial position of the tip, and progressively approaching the tip by increments of 0.1 Å. A complete geometry optimization is performed for each position of the tip, so that a local minimum is obtained. No temperature is included in the calculation, since we wish to relate with possible low temperature experiments, and electronic energies are presented. The position of the tip is referenced to the geometry of contact between the tip and the radical molecule (defined a Z = 0, point d_1 on Figure 4), where the tip apex atom creates a bond at equilibrium with the C radical (Au−C distance 1.99 Å) and which represents the minimum for the system energy. The calculation models the state of the tip-molecule system upon approach then retraction of the tip, assuming low temperature and fast atomic rearrangement in the local energy minimum with respect to the approach velocity, so that the system would be at equilibrium at any position of the tip.

If the tip is placed with its apex atom directly on-top of the carbon radical at a large separation, this apex atom is very stable with three metallic Au−Au bonds to the tip substrate and its detachment very energetically unfavorable. Upon approach, one first sees a weak long-distance interaction, the

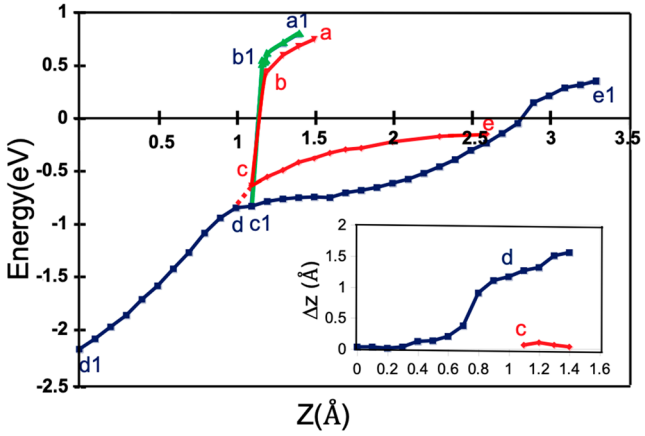

Figure 4. Energy profile (in eV) for the controlled atomic scale etching in the sharp tip model (Figure 2a) with the ethynyl-adamantane-trithiol radical bound to the Au(111) surface. The Au tip approaches toward the surface carbon radical starting from point (a) and retracts leaving one Au atom on the molecule to reach (e) or (e1). The abscissa Z coordinate represents the separation between the fixed layers of the surface and tip slab, relative to the equilibrium contact point between tip and surface (d1). The inset shows the maximum ΔZ coordinate in the Au_3 second layer of the tip (just above the abstracted tip apex atom) to show whether this Au_3 unit stays horizontal (ΔZ close to 0) or is markedly tilted to form a neck between the tip and the ethynyl group. In (a) the lowest atom of the tip is placed on top of the radical during the approach, while in (a1) a lateral offset of 0.5 Å is applied.

tip apex atom remaining in its position, resulting in a slow decrease of the energy following the red curve in Figure 4 (from position (a) to (b) in Figure 4 with corresponding structure (a) in Figure 5). An atomic movement occurs at a tip-radical separation of Z = 1.1 Å, where the barrier to detach the Au tip atom vanishes and the Au tip atom is transferred to the carbon radical, breaking three Au−Au bonds in the tip and forming one C−Au bond, to create structure (c) in Figure 5 with a stabilization of ∼1.5 eV versus (a) as shown at (c) along the red curve of Figure 4. From (c), retraction of the tip follows the red curve until (e), corresponding to the desired clean abstraction of a single atom from the Au tip. It is important to note that the interaction between the tip atom and its base is not completely canceled in structure (c), resulting in an energy increase of an additional ∼0.7 eV following complete separation by tip retraction (from (c) to (e)). It should be underlined that along the red pathway in

https://doi.org/10.1021/prechem.3c00011
Precis. Chem. 2023, 1, 119−126

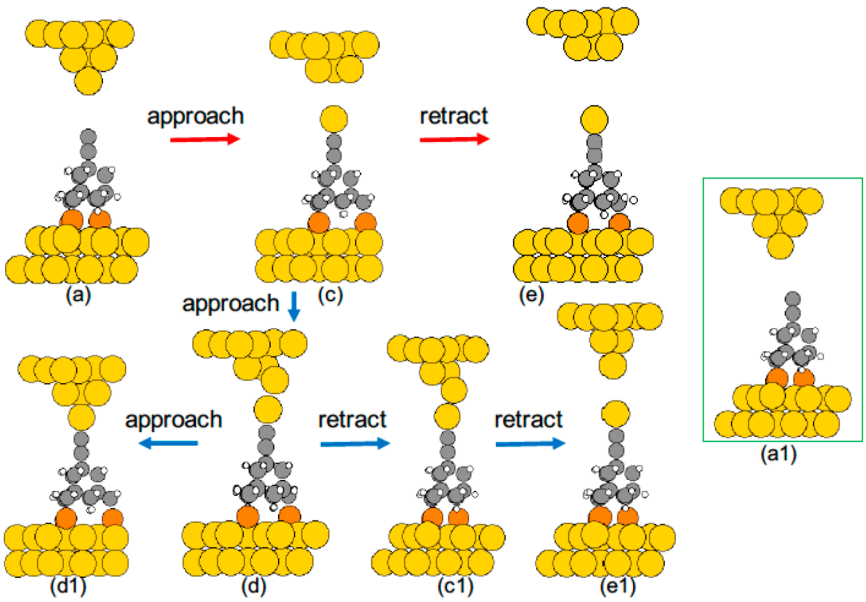

Figure 5. Geometries during the tip atom abstraction process from the sharp tip with the surface mounted ethynyl-adamantane-trithiol radical. The apical tip atom is approached directly on top of the C radical, except for (a1) where it is shifted laterally by 0.5 Å. Labels correspond to those in Figure 4 (Au: yellow; C: gray; H: white, small; S: orange). Red (blue) arrows correspond to red (blue) lines in Figure 4. Approach (retract) indicates that the tip is moved closer (further) to (from) the radical.

Figure 4, the tip Au atom is either attached to the tip base (from (a) to (b)), or to the C radical (from (c) to (e)) and is never shared between tip and radical. When the tip is retracted from (c) the Au atom remains on the C radical for two reasons: the energy is more favorable (moving back to the tip is uphill by ∼1 eV) and in addition as soon as Z is increased above 1.1 Å an energy barrier rebuilds for the migration.

This reactive process is not unique, and other pathways were observed to occur. Structure c in Figure 5 represents a local energetic minimum, where the Au_3 triangle exposed at the tip apex after transfer of the apical tip atom remains horizontal. From (c), if instead of retracting the tip, it is further approached to a tip-molecule separation of Z = 1 Å, the topology of the potential energy surface is altered. Specifically, the equivalent of (c) is no longer stable and becomes a maximum on the potential energy surface. The structure then transforms into a configuration where one atom of the Au_3 triangle moves toward the molecule and rebinds with the Au atom that had been transferred to the C radical as seen in structure (d) in Figure 5. This rebinding creates a continuous "neck" between the tip and radical, a structure which is reminiscent of the known malleable and ductile behavior of gold. The tip apex atom is then shared between the deformed tip base and the C radical. Such neck-like structures are represented on the blue curve in Figure 4 and linked by blue arrows in Figure 5. The inset of Figure 4 shows a value denoted as ΔZ, which represents the magnitude of tilt (indicated as a Z difference) in the Au triangle that forms the base of the tip. For structure (c) as well as all other points on the red curve, ΔZ is zero as the tip base remains horizontal following transfer of the Au atom from the tip to the radical. For structure (d), represented on the blue curve at Z = 1 Å, ΔZ is large since one atom of the Au_3 triangle at the tip is markedly lower (by 1.2 Å) than the other two. This ΔZ value decreases progressively as the tip moves toward the radical. At the minimal contact separation (d1, Z = 0), the tip structure is no longer deformed. All bonds are re-established within the Au tip and a bond is formed between the tip and the radical. The energy of (d1) is 2.8 eV more stable than that of the initial point (a), corresponding to the energy of Au−C bond formation at the tip apex.

If from structure (d1), we now retract the tip by increasing Z the process is not fully reversible. The same structures as those during the approach are initially observed. Moving from point (d) as ΔZ continuing to increase, the deformed neck-like structure is maintained, forming (c1) instead of (c). From (c1), a small energy increase is observed following a rearrangement in the neck, corresponding to rotation of the Au_3 triangle without Au−Au bond breaking until Z ∼ 1.6 Å where the Au_3 triangle is vertical. Abstraction of one Au atom from the tip then occurs with a corresponding increase of the energy until the formation of structure (e1), where the apex Au atom has detached from the tip and transferred onto the carbon radical. Again, the Au atoms remains on the radical C for stability reason. The tip structure after abstraction is found to be metastable in this case, with one Au atom dangling down. Subsequent reorganization of this (e1) structure to (e) is possible but requires the system to overcome a small energetic barrier (0.06 eV) that would only be kinetically possible at temperatures above ∼25 K.

Therefore, the on-top approach of a sharp tip produces two distinct isomers for the interacting tip and radical over the Z range of 1.1 to ∼2.5 Å, corresponding either to a Au apex atom fully detached from the tip base or to the formation of neck-like structures, the apex atom remaining partially bonded to other Au atoms of the tip. For Z values less or equal than 1 Å, only the neck-like structure is possible. The height of the energy barrier between these two isomers is an important parameter to determine whether both can be found. For Z = 1.1 Å, that corresponds to the tip−surface separation for which the tip atom is transferred to the radical, that barrier between (c) and (c1) is only 0.05 eV, a small value implying that the

https://doi.org/10.1021/prechem.3c00011
Precis. Chem. 2023, 1, 119−126

metastable structure (c) can only exist at low temperature, but would quickly transform to the most stable neck structure (c1) at elevated temperature.

Experimental realization of a tip-molecule approach directly and exactly on-top of the radical carbon cannot be presumed. To examine the impacts of lateral offsets between the apical tip atom and the carbon radical, the sharp tip model was used to approach with a constant lateral shift of 0.5 Å. Such an offset is readily achievable with SPM-based methods. The starting point of the offset trajectory is noted as (a1) in Figure 4 (green) and in the inset of Figure 5. The approach is unreactive until (b1), where the tip atom transfers across the gap to form a bond with the C radical in a process similar to that of the on-top approach. The difference with the on-top approach is that a structure like (c) with the Au apex atom fully detached is not seen and the remaining atoms of the tip rearrange in this offset case to form a neck-like structure very similar to (c1), with an important tilt of the Au_3 triangle at the tip. Upon retraction of the tip, structures similar to those observed in the case of the on-top approach following the neck formation (blue curve in Figure 4) are formed, resulting in the abstraction of a single Au atom from the tip.

c. Atom Abstraction from the Blunt Tip Model with the Ethynyl-Adamantane-Trithiol Radical

The sharp tip model cannot be presumed during the course of any SPM experiment. Similarly, the sequential abstraction of atoms from the tip will necessarily produce tip apex structures that can be best described as "blunt", where for example the apex structure of the blunt tip is terminated with three atoms in the same plane, as shown in Figure 5c and e. To explore the possibility of sequential atom abstraction, a blunt tip model was developed (Figure 2b) and one Au atom at the Au_3 apex was positioned for a vertical on-top approach toward the radical. The associated energy profiles and structural descriptions for this reaction trajectory are provided in Figures 6 and 7, respectively. The Z coordinate of the tip is again referenced to the contact situation; however, two different contact geometries are found depending of the lateral position of the C atom of the radical, on-top of one Au atom, or in between 3 Au atoms. The one corresponding to the lowest tip position (in between 3 Au atoms, structure F1 on Figure 7) has been selected.

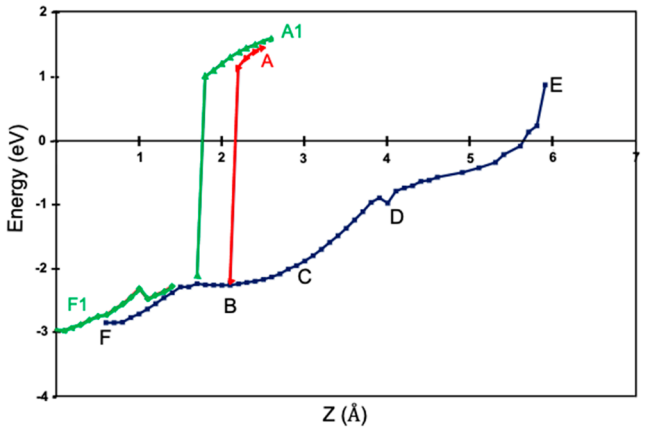

Figure 6. Energy profile (in eV) for the controlled atomic scale etching of the blunt tip model with the ethynyl-adamantane-trithiol radical mounted on a Au(111) surface. The Au tip approaches toward the surface carbon radical starting from points A or A1 and retracts leaving one Au atom on the molecule to reach E. The abscissa Z coordinate represents the separation between the fixed layers of the surface and tip slab, relative to lowest value obtained for the equilibrium contact point F1 between tip and surface.

Beginning from structure (A), approach of one Au atom at the Au_3 apex on top of the radical results in reorganization of the tip apex at Z = 2.1 Å, where the Au atom above the radical moves to bond with the radical while remaining bonded to the two other Au atoms of the tip in a process that lowers the energy by more than 2 eV (Figure 6). This observation is markedly different from the case of the sharp tip model, where the abstracted atom in structure (c) of Figure 5 was completely detached from the tip. The presence of three atoms at the same Z position in the blunt tip model allows for two of the atoms to remain bonded to the atom that is ultimately abstracted leading to the formation of a neck-like structure, similar to the case seen in Figure 5d or c1. These additional interactions during atom abstraction make the process more energetically favorable and the resultant structure more stable relative to the energy zero.

Therefore, from structure (B) in Figure 7, retraction of the tip results in formation of a monatomic neck of Au between the radical and the tip as shown in Figure 7(C) and (D). At Z ~ 5.5 Å the neck breaks, one Au atom remaining on the radical and a metastable structure being formed for the remaining of the tip apex (Figure 7E), that can rearrange at finite temperature by rebinding one atom to the base. In contrast, continuation of the tip approach from structure (B) results in reorganization of the tip and a return to its initial configuration denoted as structure (F), where the radical is bonded to one atom of the intact Au_3 blunt tip.

To again consider the effects of lateral offsets between the Au atoms in the tip and the carbon radical, approach of the tip was initiated from structure (A1), where the center of the triangular tip apex was positioned above the radical. The resulting process lead to very similar results. During approach, the surface-bound molecule bends slightly to allow for increased interaction between the end carbon atom with one of the three Au atoms at the tip apex. At a sufficiently short separation, the interacting Au atom spontaneously jumps to the radical carbon and produces a structure very similar to (B). Continuation of the approach until contact results in structure (F1), with the radical carbon symmetrically placed below the center of the tip Au_3 triangle. Retraction of the tip follows structure very similar to (B, C, D, E) so that the exact position of the tip with respect to the carbon radical has little importance for Au atom abstraction result.

d. Atom Abstraction Trajectories from the Sharp Tip with the Adamantyl-Trithiol Radical

To explore the influence of interaction strength between the carbon radical and apical Au atoms, a second molecular tool was employed. Removal of the ethynyl fragment from the molecular structure allowed for formation of the radical directly at the adamantane carbon (Scheme 1b), thereby changing from an sp carbon radical to an sp^3 carbon radical, the latter of which is known to be less reactive. Using the sharp tip model, the resulting abstraction process was observed to be less energetically favorable. Specifically, the overall process becomes slightly uphill in energy (Figure 8), in contrast to the markedly favorable process using an ethynyl radical previously seen in Figure 4.

https://doi.org/10.1021/prechem.3c00011
Precis. Chem. 2023, 1, 119−126

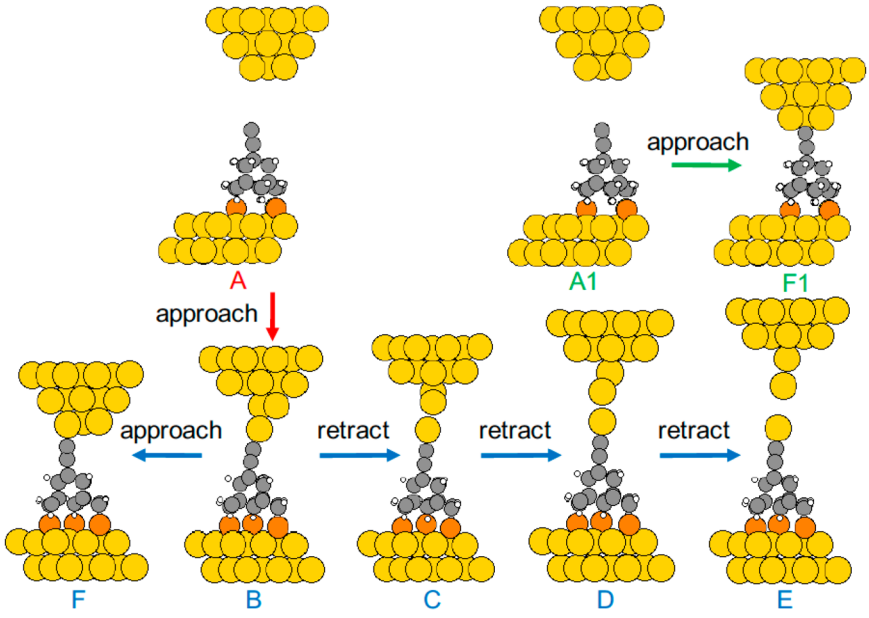

Figure 7. Geometries during the tip atom abstraction process from the blunt tip with the surface-bound ethynyl-adamantane-trithiol radical. In (A), one atom of the Au_3 tip apex is positioned directly above the carbon radical. Tip approach produces a Au neck between the tip and molecule (B). Subsequent retraction of the tip (C, D, then E) leads to the detachment of the tip Au atom and to the formation of a metastable structure at the tip apex. Further approach from (B) leads to the contact structure (F). In A1, the center of the tip is positioned above the radical during approach. The corresponding contact structure is denoted as (F1). Arrow colors refer to the energy curves and labels in Figure 6.

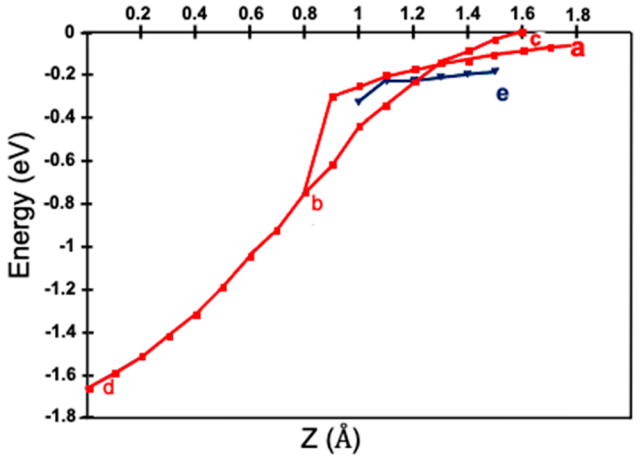

Figure 8. Reaction trajectory for the tip atom abstraction process from the sharp tip with an adamantane-trithiol based sp^3-C radical. Energy vs displacement graph is shown. Labels refer to structures in Figure 9.

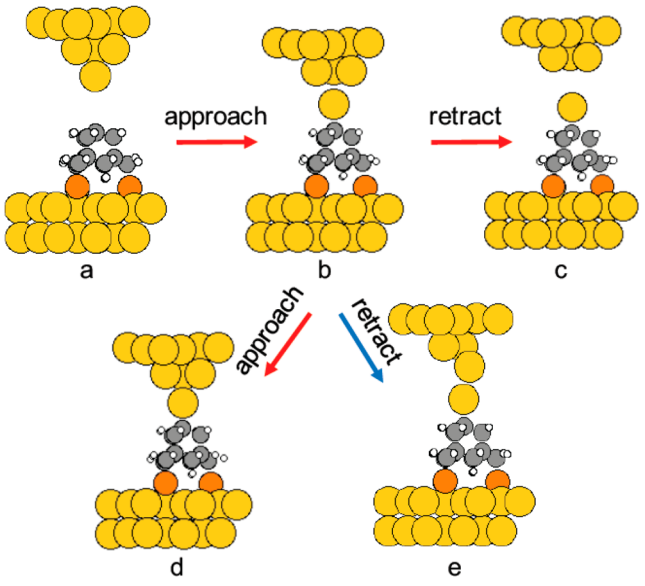

Figure 9. Geometries during the tip atom abstraction process from the sharp tip with the surface mounted adamantyl-trithiol radical. The apical tip atom is approached directly on top of the C radical. Labels (a)−(e) correspond to those in Figure 8 (Au: yellow; C: gray; H: white, small; S: orange). Red (blue) arrows correspond to red (blue) lines in Figure 8. Approach (retract) indicates that the tip is moved closer (further) to (from) the radical.

Whether the atom abstraction process can still occur in the case of the adamantyl trithiol radical despite the slightly unfavorable energetic balance was examined by positioning the apical Au tip atom of the sharp tip model directly on-top of the carbon radical center as shown in Figure 9 (a). The zero of the tip-molecule separation is again set at the equilibrium contact position. Upon progressive approach, the Au tip atom is transferred toward the radical at Z = 0.8 Å and with an associated energy drop of 0.5 eV to produce structure (b) (Figure 9b). The separation at which the barrier for Au atom transfer vanishes is hence 0.3 Å shorter than in the previous case of the ethynyl-adamantane-trithiol radical, while the energy change is approximately a third (see Figure 4). This is all in clear link with the much less energetically favored atom transfer for this adamantyl trithiol radical. At this Z = 0.8 Å tip-molecule separation, an Au−C bond is formed alongside elongation of Au−Au bonds at the tip. By retracting the tip from (b), the complete detachment of the Au tip atom can be obtained and requires an energy of 0.75 eV, reaching structure (c) with the gold atom on the radical (Figure 9c). The overall process from (a) to (c) is slightly energy uphill, which requires

https://doi.org/10.1021/prechem.3c00011
Precis. Chem. 2023, 1, 119−126

external work provided by the manual retraction sequence to transfer the tip-atom to the radical. Interestingly, while the bond between the C radical and the Au atom has a slightly lower energy than the bond between the Au tip atom and base, the process of atom abstraction from the tip and transfer to the radical is observed to be nonreversible. Reapproach of the Au_3 tip base toward the transferred Au atom stabilizes the system by reformation of Au−Au bonds, resulting in structure (b). Continued approach ultimately yields structure (d) (Figure 9d), which represents the energy minimum where all Au−C and Au−Au bonds have been established. Retraction of the tip from (d) leads to elongation of Au−Au bonds within the tip that are easier to elongate as compared to the Au−C bond between the tip and radical. Continued retraction of the tip beyond structure (b) follows the lower energy trajectory leading to (c) in Figure 8. For $Z > 1.3$ Å, switching to the line leading to (a) is thermodynamically possible, but requires a long distance jump of the gold atom from the radical to the tip, which is activated and kinetically hindered at low temperature. The system therefore remains on the metastable structure with the Au atom on the C radical. The Au atom is hence kinetically trapped on the C radical and is not back transferred to the Au tip, despite the fact that this process would be slightly energetically favored.

Another path can compete with the red pathway, consisting of the formation of a "Au neck", shown as the blue path on Figure 8, and structure e on Figure 9. From Figure 8, the formation of these structures with a Au neck (blue line) is not energetically favored until $Z > 1.2$ Å and even then would be required to pass a small barrier. As a result, at low temperature, from (b) the system would continue on the line toward (c) forming metastable states, i.e., the structures with neck would not be formed. At a higher temperature, the structures with neck would be formed as (e) on Figure 9. From (e), further separation of the tip would detach the terminal tip atom as seen before.

CONCLUSION

First-principles atomistic simulations have been used to explore the feasibility of atomically controlled abstraction of atoms from an Au tip by mechanochemical means using surface-bound carbon radicals as a molecular tool. Such radicals can be obtained by activation of halogenated molecules using photon excitation or inelastic tunneling. Using two model systems, ethynyl-adamantane-trithiol and adamantyl-trithiol radicals, we demonstrate the feasibility of controlled atomic abstraction by approach and retraction of the tip apex from the radical species. The atom transfer is both distance-dependent and abrupt, occurring at a threshold distance and with an energy drop of ∼0.5−2 eV, depending of the radical species and on the structure of the Au tip apex. Two distinct states are observed following atom transfer: (1) the transferred Au atom is detached from the tip and remains only bound to the C radical, and (2) the tip apex rearranges to form a continuous neck-like structure between the radical and the tip, so that the transferred Au atom remains bonded to other Au atoms of the tip. In the latter case, retraction of the tip leads to detachment of the Au atom that remains bound to the radical. The lateral position of the tip versus the radical center is also shown to be important, as small lateral shifts from the on-top position can lead to the formation of a neck-like structure between the tip and the radical. Consideration of a "flatter" tip with three Au atoms in the apical layer also results in Au atom abstraction, however the immediate detachment upon approach is not seen. An atom transfer is found, with even stronger energy gain, but only the structure with neck formation occurs. This is due to the fact that the transferred Au atom keeps bonding with the other two Au atoms in the lowest layer of the tip, a configuration not possible for the sharp tip. Single Au atom abstraction can nevertheless occur upon retraction of the tip.

Changing the radical to a less reactive one as adamantyl trithiol makes the atom process slightly energetically unfavorable, but still possible if the tip exerts some work. Interestingly, the formation of a Au neck upon transfer is less favorable than the net transfer of the Au atom so that the weaker radical could help for a cleaner atom extraction from the tip, without deformation of other atom positions at the tip.

Once the radical has interacted with the metallic tip, the abstracted Au atom is strongly attached to the radical and that Au atom does not need to be removed nor does the molecule need to be reused to continue the atomic etching process of the tip. Sublimation of the molecules will deposit many molecules on the surface which can be used for sequential steps. This can range from very low, submonolayer coverages to monolayers, thereby providing anywhere from 10−100's of molecules up to millions. Although the results here have been obtained from specific examples, they can be extended to other couples of tip/radicals by scaling the bond energies. Our calculations open a route to the design of systems for atomically precise atom removal from metallic tips.

AUTHOR INFORMATION

Corresponding Author

Philippe Sautet − *Chemical and Biomolecular Engineering Department and Chemistry and Biochemistry Department, University of California, Los Angeles, Los Angeles, California 90095, United States; California NanoSystems Institute, University of California, Los Angeles, Los Angeles, California 90095, United States;* orcid.org/0000-0002-8444-3348; Email: sautet@ucla.edu

Authors

Pallavi Bothra − *Chemical and Biomolecular Engineering Department, University of California, Los Angeles, Los Angeles, California 90095, United States; California NanoSystems Institute, University of California, Los Angeles, Los Angeles, California 90095, United States*

Adam Z. Stieg − *California NanoSystems Institute, University of California, Los Angeles, Los Angeles, California 90095, United States*

James K. Gimzewski − *California NanoSystems Institute, University of California, Los Angeles, Los Angeles, California 90095, United States; Chemistry and Biochemistry Department, University of California, Los Angeles, Los Angeles, California 90095, United States*

Complete contact information is available at: https://pubs.acs.org/10.1021/prechem.3c00011

Notes

The authors declare no competing financial interest.

ACKNOWLEDGMENTS

This research has been funded by the US Department of Energy, Office of Energy Efficiency and Renewable Energy

under Award Number DE-EE0008308. The computer time was funded by the Extreme Science and Engineering Discovery Environment (XSEDE), which is supported by National Science Foundation Grant Number TG-CHE170060.[25] Specifically, it used the Bridges, Bridges-2 (Pittsburgh Supercomputing Center (PSC)), and SDSC Expanse compute systems.

REFERENCES

(1) Fuechsle, M.; Miwa, J.; Mahapatra, S.; Ryu, H.; Lee, S.; Warschkow, O.; Hollenberg, L. C. L.; Klimeck, G.; Simmons, M. Y. A single-atom transistor. *Nat. Nanotechnol.* **2012**, *7*, 242−246.
(2) Eigler, D. M.; Schweizer, E. K. Positioning single atoms with a scanning tunnelling microscope. *Nature* **1990**, *344*, 524−526.
(3) Jesse, S.; Borisevich, A. Y.; Fowlkes, J. D.; Lupini, A. R.; Rack, P. D.; Unocic, R. R.; Sumpter, B. G.; Kalinin, S. V.; Belianinov, A.; Ovchinnikova, O. S. Directing matter: toward atomic-scale 3D nanofabrication. *ACS Nano* **2016**, *10*, 5600−5618.
(4) Umbrello, S.; Baum, S. D. Evaluating future nanotechnology: The net societal impacts of atomically precise manufacturing. *Futures* **2018**, *100*, 63−73.
(5) Meyer, G.; Zöphel, S.; Rieder, K. H. Manipulation of atoms and molecules with a low temperature scanning tunneling microscope. *Appl. Phys. A: Mater. Sci. Process.* **1996**, *63*, 557−564.
(6) Bartels, L.; Meyer, G.; Rieder, K. H. Controlled vertical manipulation of single CO molecules with the scanning tunneling microscope: A route to chemical contrast. *Appl. Phys. Lett.* **1997**, *71*, 213−215.
(7) Dujardin, G.; Mayne, A.; Robert, O.; Rose, F.; Joachim, C.; Tang, H. Vertical Manipulation of Individual Atoms by a Direct STM Tip-Surface Contact on Ge(111). *Phys. Rev. Lett.* **1998**, *80*, 3085−3088.
(8) Shen, T.-C.; Wang, C.; Abeln, G. C.; Tucker, J. R.; Lyding, J. W.; Avouris, P.; Walkup, R. E. Atomic scale desorption through electronic and vibrational excitation mechanisms. *Science* **1995**, *268*, 1590−1592.
(9) Hersam, M. C.; Guisinger, N. P.; Lyding, J. W. Silicon based molecular nanotechnology. *Nanotechnology* **2000**, *11*, 70−76.
(10) Møller, M.; Jarvis, S. P.; Guérinet, L.; Sharp, P.; Woolley, R.; Rahe, P.; Moriarty, P. Automated extraction of single H atoms with STM: Tip state dependency. *Nanotechnology* **2017**, *28*, 075302.
(11) Gretz, O.; Weymouth, A. J.; Giessibl, F. J. Identifying the atomic configuration of the tip apex using STM and frequency-modulation AFM with CO on Pt(111). *Phys. Rev. Research* **2020**, *2*, 033094.
(12) Welker, J.; Giessibl, F. J. Revealing the Angular Symmetry of Chemical Bonds by Atomic Force Microscopy. *Science* **2012**, *336*, 444.
(13) Kresse, G.; Hafner, J. Ab initio molecular dynamics for liquid metals. *Phys. Rev. B* **1993**, *47*, 558.
(14) Perdew, J. P.; Burke, K.; Ernzerhof, M. Generalized gradient approximation made simple. *Phys. Rev. Lett.* **1996**, *77*, 3865.
(15) Grimme, S.; Antony, J.; Ehrlich, S.; Krieg, S. A consistent and accurate ab initio parametrization of density functional dispersion correction (DFT-D) for the 94 elements H-Pu. *J. Chem. Phys.* **2010**, *132*, 154104.
(16) Love, J. C.; Estroff, L. A.; Kriebel, J. K.; Nuzzo, R. G.; Whitesides, G. M. Self-Assembled monolayers of thiolates on metals as a form of nanotechnology. *Chem. Rev.* **2005**, *105*, 1103−1170.
(17) Poirier, G. E. Characterization of organosulfur molecular monolayers on Au(111) using scanning tunneling microscopy. *Chem. Rev.* **1997**, *97*, 1117−1128.
(18) Salmeron, M.; Neubauer, G.; Folch, A.; Tomitori, M.; Ogletree, D. F.; Sautet, P. Viscoelastic and Electrical Properties of Alkylthiol Monolayers on Au(111) Films. *Langmuir* **1993**, *9*, 3600−3611.
(19) Thomas, J. C.; Goronzy, D. P.; Serino, A. C.; Auluck, H. S.; Irving, O. R.; Jimenez-Izal, E.; Deirmenjian, J. M.; Macháček, J.; Sautet, P.; Alexandrova, A. N.; Baše, T.; Weiss, P. S. Acid−base control of valency within carboranedithiol self-assembled monolayers: molecules do the can-can. *ACS Nano* **2018**, *12*, 2211−2221.
(20) Mom, R. V.; Melissen, S. T. A. G.; Sautet, P.; Frenken, J. W. M.; Steinmann, S. N.; Groot, I. M. N. The pressure gap for thiols: methanethiol self-assembly on Au(111) from vacuum to 1 bar. *J. Phys. Chem. C* **2019**, *123*, 12382−12389.
(21) Qi, Y.; Qin, J.; Zhang, G.; Zhang, T. Breaking mechanism of single molecular junctions formed by octanedithiol molecules and Au electrodes. *J. Am. Chem. Soc.* **2009**, *131*, 16418−16422.
(22) Batista, R. J. C; Ordejón, P.; Chacham, H.; Artacho, E. Resistive and rectifying effects of pulling gold atoms at thiol-gold nanocontacts. *Phys. Rev. B* **2007**, *75*, 041402.
(23) Katano, S.; Kim, Y.; Matsubara, H.; Kitagawa, T.; Kawai, M. Hierarchical chiral framework based on a rigid adamantane tripod on Au(111). *J. Am. Chem. Soc.* **2007**, *129*, 2511−2515.
(24) Katano, S.; Kim, Y.; Kitagawa, T.; Kawai, M. Tailoring electronic states of a single molecule using adamantane-based molecular tripods. *Phys. Chem. Chem. Phys.* **2013**, *15*, 14229−14233.
(25) Towns, J.; Cockerill, T.; Dahan, M.; Foster, I.; Gaither, K.; Grimshaw, A.; Hazlewood, V.; Lathrop, S.; Lifka, D.; Peterson, G. D.; Roskies, R.; Scott, J. R.; Wilkins-Diehr, N. Xsede: accelerating scientific discovery. *Computing in science& engineering* **2014**, *16*, 62−74.

https://doi.org/10.1021/prechem.3c00011
Precis. Chem. 2023, 1, 119−126